Defect Processes in a PbS Metal Organic Framework: A Quantum-Confined Hybrid Semiconductor

ARTICLE *in* JOURNAL OF PHYSICAL CHEMISTRY LETTERS · MARCH 2010

Impact Factor: 7.46 · DOI: 10.1021/jz100312y

1 AUTHOR:

Aron Walsh
University of Bath
203 PUBLICATIONS **6,001** CITATIONS

THE JOURNAL OF PHYSICAL CHEMISTRY Letters

pubs.acs.org/JPCL

Defect Processes in a PbS Metal Organic Framework: A Quantum-Confined Hybrid Semiconductor

Aron Walsh*

University College London, Department of Chemistry, Materials Chemistry, Third Floor, Kathleen Lonsdale Building, Gower Street, London WC1E 6BT, United Kingdom

ABSTRACT We report the effects of reduced dimensionality and organic networks on defect reactions in a hybrid solid of PbS (galena). Through first-principles calculations, we demonstrate that formation of the organic−inorganic network increases both the band gap and defect reaction energies. Remarkably, anion vacancies result in a localized defect center in both the bulk and hybrid materials, with high ionization energies deep in the band gap, while cation vacancies provide low energy shallow acceptor levels; the hybrid system will favor intrinsic *p*-type conductivity. The results demonstrate the feasibility of utilizing hybrid solids to engineer material properties for solar cell applications.

SECTION Electron Transport, Optical and Electronic Devices, Hard Matter

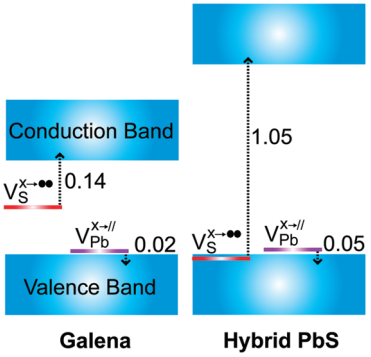

Metal organic frameworks (MOFs) have emerged at the interface between organic and inorganic materials chemistry.[1,2] The majority of MOF research has been centered on open framework structures with potential for gas storage and catalysis, the hybrid analogues of porous zeolites.[3] Hybrid systems containing higher dimensionality in the inorganic networks have demonstrated novel anisotropic electronic, magnetic, and optical effects.[4−6] Interfaces between organic and inorganic materials are presently exploited in organic solar cell and light emission devices, and the integration of similar features into a crystalline hybrid material offers immense potential for functional property engineering.

In this letter, we take an archetypal binary semiconductor with excellent electron transport properties, PbS, which has shown potential for application in high efficiency "third-generation" solar cells,[7] and investigate changes in the electronic structure and defect processes on the formation of a hybrid organic−inorganic PbS solid, through density functional theory (DFT) calculations. The hybrid material, which was recently synthesized by Turner et al.,[8] preserves PbS bonding in three dimensions and was found to have an optical band gap of 1.7 eV, ideal for harvesting the visible spectrum for photocatalytic and photovoltaic applications.

PbS is a narrow band gap (0.42 eV) semiconductor that has attracted significant attention for quantum dot and multiple-exciton-generation (MEG) solar cells,[9,10] and adopts a centrosymmetric rock-salt lattice with $a = 5.936$ Å,[11] as shown in Figure 1. The calculated lattice constant of PbS is 6.006 Å, at the generalized gradient approximation (GGA)-DFT level, within 1.5% of experiment. The electronic density of states of PbS is shown in Figure 2. The occupied Pb 6s band is present between −6 and −8 eV, with evidence of some hybridization of S 3p, consistent with previous analysis.[12,13] The GGA fundamental band gap is direct at the L point of the first Brillouin zone (0.47 eV), with the conduction band composed predominately of Pb 6p states. The inclusion of spin−orbit coupling, which is not presently considered, lowers the degeneracy of the empty 6*p* band, but does not significantly affect the band structure.[13]

The crystal structure of the hybrid PbS system, $Pb_3(C_6S_6)$, is hexagonal (*P6*/*mmm*) and consists of alternating planes of Pb and S/C oriented along the [0001] direction. Each Pb atom lies at the center of a cube with 8-fold sulfur coordination, while each S atom is coordinated to four lead and one carbon atom. The carbon atoms form sulfur-terminated planar hexagonal rings, i.e., a derivative of benzenehexathiol. The equilibrium GGA-DFT structural parameters contain errors of less than 1.5%, as listed in Table 1. The electronic density of states shows significant differences in comparison to bulk PbS. The sulfur states in the valence band become broadened as a result of the addition of interactions between C and S. Of particular note are a localized peak at −9.5 eV (π bonding between C and S) and a peak at the top of the valence band (π^* antibonding). The Pb states remain largely unchanged, with the presence of a Pb 6s-derived peak below −8 eV. In contrast, reduction of the PbS connectivity increases the fundamental band gap to 1 eV; the large excition Bohr radius of PbS makes its susceptible to quantum confinement effects, and a similar band gap is approached with a nanoparticle size of 5 nm.[14] The difference between the calculated band gap and the experimentally determined optical gap of 1.7 eV

Received Date: March 10, 2010
Accepted Date: March 26, 2010

DOI: 10.1021/jz100312y | *J. Phys. Chem. Lett.* **2010**, *1*, 1284–1287

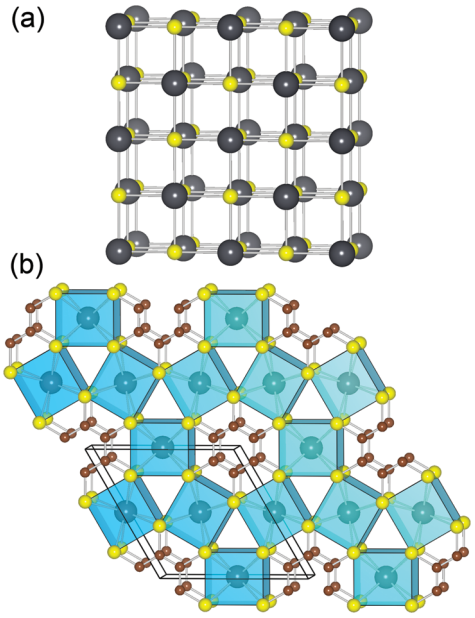

Figure 1. Crystal structure representations of (a) rock-salt PbS and (b) $Pb_3(C_6S_6)$. The carbon atoms are colored brown, with gray Pb and yellow S. In the hybrid system, the PbS cubes are shaded blue.

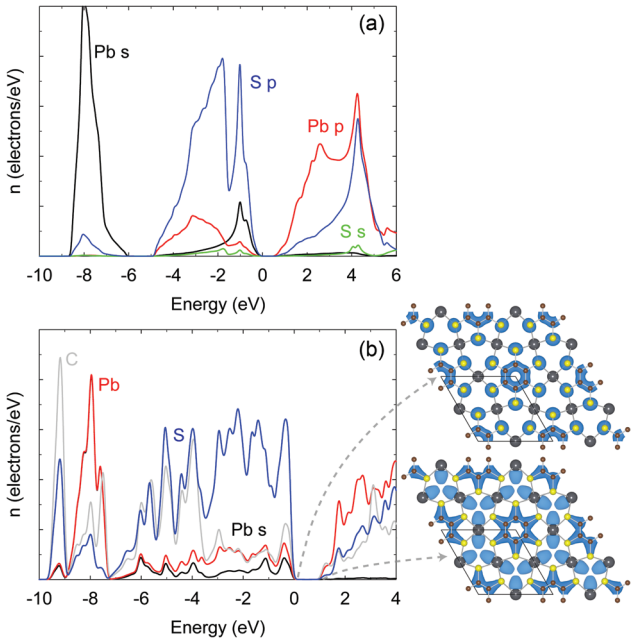

Figure 2. Site-projected electronic density of states of (a) rock-salt PbS and (b) hybrid PbS. The highest occupied state is set to 0 eV. Electron density isosurfaces for the band edge states in the hybrid material are shown in blue.

arises through a combination of the intrinsic limitations of the GGA-DFT exchange-correlation functional and the approximate nature of the experimental extrapolation of the visible light absorption onset.[8]

Critical to the physicochemical properties of any material is the underlying defect chemistry. To this end, we investigate the formation of a Schottky pair in the inorganic network, including its two constituent species: vacant anion and cation lattice sites. Defect formation energies were obtained from $\Delta E_f = [E_{defect} - E_{host}] + \mu_\alpha$, where E_{defect} and E_{host} are the total energies of the defective and bulk systems, performed with equivalent k-point sampling and basis sets. The chemical potential of the removed species (μ_α) are taken with respect to the elements in their standard states, i.e., bulk Pb and S solids. The first two point defect reactions considered are the formation of neutral anion and cation vacancies, namely,

$$S_S \rightleftharpoons V_S^x + S(s)$$

and

$$Pb_{Pb} \rightleftharpoons V_{Pb}^x + Pb(s)$$

using the standard notation of Kröger and Vink. In bulk PbS, the cost of anion and cation vacancy formation is 1.77 and 1.36 eV, respectively. The corresponding neutral Schottky formation energy is remarkably low at 1.04 eV per defect, suggesting that it will be a predominant form of ionic disorder (see Table 2). The electron/hole density associated with the defect bands are plotted in Figure 3: the Pb vacancy results in a delocalized hole state, and the S vacancy results in an F-center (or color center), with the majority of the two excess electrons localized on the vacancy center, accompanied by polarization of the neighboring Pb sites. In the hybrid material, the anion vacancy remains higher in energy than the cation vacancy; however, both values are increased from those in bulk PbS. This is illustrated by the energy required to create a Schottky pair, which is increased to 1.58 eV. Again the defect charge density is associated with a localized center for the S vacancy, which spills into the neighboring π-framework, with a more delocalized hole state for the Pb vacancy, as illustrated in Figure 4.

Table 1. The Equilibrium GGA-DFT Structural and Electronic Parameters of the Bulk and Hybrid PbS Systems[a]

	bulk PbS	hybrid PbS
a (Å)	6.006 (5.936)	9.053 (8.964)
b (Å)		
c (Å)		4.006 (3.958)
α (deg)	90	90
β (deg)	90	90
γ (deg)	90	120
Pb−S (Å)	6 × 3.00	8 × 3.11
E_g (eV)	0.47 (0.42)	0.99 (1.7)

[a] The corresponding experimental values[8,11] are shown in parentheses.

Ionization of the point defects is of importance for generating free electrical carriers, and creating luminescent centers, which for cation vacancies will result in free electron holes,

$$V_{Pb}^x \rightleftharpoons V_{Pb}^{//} + 2h^\bullet$$

DOI: 10.1021/jz100312y | J. Phys. Chem. Lett. 2010, 1, 1284–1287

Table 2. Defect Reaction Energies[a]

defect reaction	bulk PbS	hybrid PbS
$S_S \rightleftharpoons V_S^x + S(s)$	1.77	2.47
$V_S^x \rightleftharpoons V_S^{\bullet\bullet} + 2e'$	0.14	1.05
$Pb_{Pb} \rightleftharpoons V_{Pb}^x + Pb(s)$	1.36	1.74
$V_{Pb}^x \rightleftharpoons V_{Pb}'' + 2h^{\bullet}$	0.02	0.05
$Pb_{Pb} + S_S \rightleftharpoons V_{Pb}^x + V_S^x + PbS(s)$	1.04	1.58
$Pb_{Pb} + S_S \rightleftharpoons V_{Pb}'' + V_S^{\bullet\bullet} + PbS(s)$	0.69	1.55

[a] All values are in eV per defect, or per electron/hole for both ionization reactions. For the hybrid material, the Schottky reaction is balanced through the precipitation of bulk PbS.

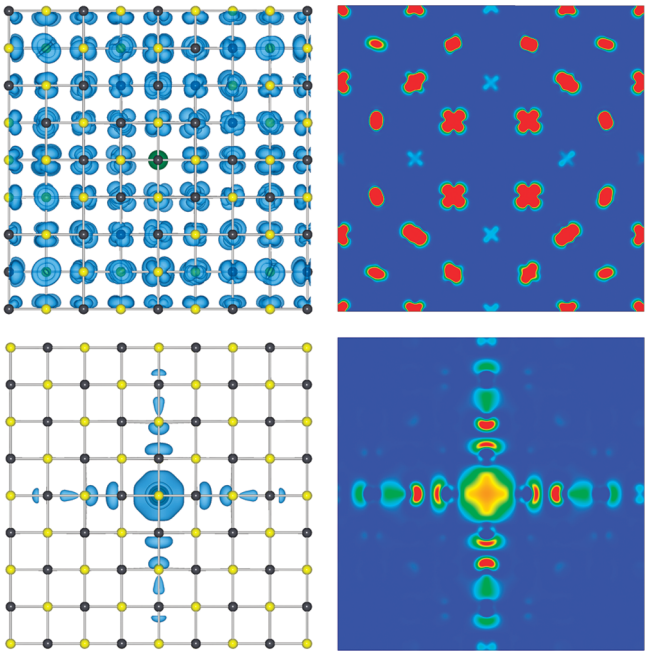

Figure 3. Density isosurfaces and contour maps arising from the hole and electron states for neutral cation (top panel) and anion (lower panel) vacancies in PbS, plotted through a (001) plane. The vacancy sites are filled with a green ball, and the contour maps are plotted from blue (0) to red (1 meV/Å^3).

and for anion vacancies will result in conduction band electrons,

$$V_S^x \rightleftharpoons V_S^{\bullet\bullet} + 2e'$$

As expected from the delocalized wave functions, the Pb vacancy is a shallow acceptor in both PbS (0.02 eV) and the hybrid material (0.05 eV), while the S vacancy has deep donor levels of 0.14 and 1.05 eV, respectively, with the latter being resonant within the upper valence band. The associated energy

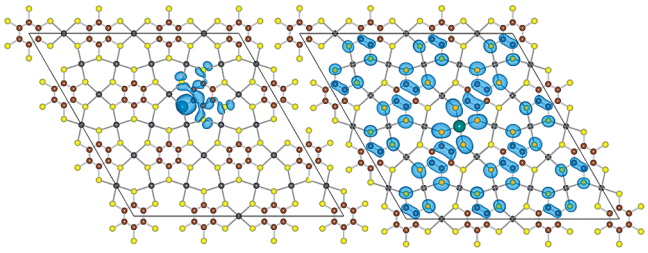

Figure 4. Density isosurfaces arising from the electron and hole states for anion (left panel) and cation (right panel) vacancies in the hybrid PbS material. The vacancy sites are filled with a green ball.

for charged Schottky pair formation is decreased to 0.74 eV for bulk PbS, and to 1.55 eV for the hybrid system; charged disorder is stabilized as a result of electron transfer between the donor and acceptor states.

On the basis of the present calculations, Schottky ionic disorder is feasible in both the bulk and hybrid PbS materials; furthermore, because of the low formation energies and shallow ionization levels for cation vacancies, we anticipate that the hybrid material will exhibit a preference for intrinsic *p*-type behavior. The hybrid system therefore maintains the key bulk material characteristics, while giving a band gap comparable to 5 nm PbS quatum dots. Further flexibility can be provided through manipulating the dimensionality of the inorganic network, with 1D, 2D, and 3D hybrid networks reported,[8] or through engineering of the component chemical species. The presence of two distinct networks offers immense chemical freedom for property engineering, in particular, for overcoming the carrier extraction bottleneck currently limiting the efficiencies of MEG solar cells.[9]

In conclusion, formation of a hybrid PbS solid maintains many of the key characteristics present in PbS, while opening up the electronic band gap similar to quantum-confined PbS nanoparticles. Schottky ionic disorder remains competitive in the hybrid structure, and the component defects have similar electronic levels to bulk PbS, with the cation vacancy acting as a shallow electron acceptor, and the anion vacancy as a deep electron donor. It remains to be seen whether this and releated hybrid materials, which contain reduced dimensionality in the PbS networks, will exhibit the beneficial effects of MEG previously demonstrated for PbS quantum dots. The potential of hybrid materials as functional optoelectronic materials remains to be exploited..

THEORETICAL SECTION

The electronic structure and total energy were calculated using DFT[15,16] within the VASP[17,18] code. Exchange-correlation effects were treated at the GGA level, namely the Perdew–Burke–Ernzerhof (PBE) functional.[19] A plane wave basis set was employed with the projector augmented wave (PAW) method[20] used to represent the valence–core (Pb:[Xe], C:[He], N:[He], S:[Ne]) interactions. Scalar-relativistic contributions are explicitly included in the PAW potentials, while spin–orbit coupling is not treated. The plane-wave cutoff (500 eV) and the *k*-point sampling were both checked for convergence.

DOI: 10.1021/jz100312y | *J. Phys. Chem. Lett.* 2010, *1*, 1284–1287

Isochoric point defect formation was investigated using 4 × 4 × 4 (512 atom) and 3 × 3 × 3 (405 atom) supercells for bulk and hybrid PbS, respectively. The defect calculations were performed using *k*-point sampling at the Γ point in a cell with P1 symmetry. For the ionized vacancy centers, the total energies of the charged unit cells were corrected through alignment of the core levels, as detailed elsewhere.[21,22] Considering the high dielectric constant (ε_0 = 170 for PbS) and the large supercell size employed (r_{defect} = 24 Å), further electrostatic corrections to the ionization reactions have been neglected.

AUTHOR INFORMATION

Corresponding Author:

*To whom correspondence should be addressed. E-mail: a.walsh@ucl.ac.uk.

ACKNOWLEDGMENT I would like to acknowledge useful discussions with C. R. A. Catlow, as well as funding from a Marie-Curie Intra-European Fellowship from the European Union. Via membership of the U.K.'s HPC Materials Chemistry Consortium, which is funded by EPSRC (EP/F067496), this work made use of the facilities of HECToR, the U.K.'s national high-performance computing service.

REFERENCES

(1) Cheetham, A. K.; Rao, C. N. R. Materials Science: There's Room in the Middle. *Science* **2007,** *318*, 58.
(2) Ferey, G. Microporous Solids: From Organically Templated Inorganic Skeletons to Hybrid Frameworks...Ecumenism in Chemistry. *Chem. Mater.* **2001,** *13*, 3084.
(3) Mellot-Draznieks, C. Role of Computer Simulations in Structure Prediction and Structure Determination: From Molecular Compounds to Hybrid Frameworks. *J. Mater. Chem.* **2007,** *17*, 4348.
(4) Huang, X.; Roushan, M.; Emge, Thomas J.; Bi, W.; Thiagarajan, S.; Cheng, J.-H.; Yang, R.; Li, J. Flexible Hybrid Semiconductors with Low Thermal Conductivity: The Role of Organic Diamines. *Angew. Chem., Int. Ed.* **2009,** *48*, 7871.
(5) Guo, Z.; Cao, R.; Wang, X.; Li, H.; Yuan, W.; Wang, G.; Wu, H.; Li, J. A Multifunctional 3D Ferroelectric and NLO-Active Porous Metal-Organic Framework. *J. Am. Chem. Soc.* **2009,** *131*, 6894.
(6) Lin, H.; Maggard, P. A. Copper(I)-Rhenate Hybrids: Syntheses, Structures, and Optical Properties. *Inorg. Chem.* **2007,** *46*, 1283.
(7) Ellingson, R. J.; Beard, M. C.; Johnson, J. C.; Yu, P.; Micic, O. I.; Nozik, A. J.; Shabaev, A.; Efros, A. L. Highly Efficient Multiple Exciton Generation in Colloidal PbSe and PbS Quantum Dots. *Nano Lett.* **2005,** *5*, 865.
(8) Turner, D. L.; Vaid, T. P.; Stephens, P. W.; Stone, K. H.; DiPasquale, A. G.; Rheingold, A. L. Semiconducting Lead-Sulfur-Organic Network Solids. *J. Am. Chem. Soc.* **2008,** *130*, 14.
(9) Talapin, D. V.; Lee, J.-S.; Kovalenko, M. V.; Shevchenko, E. V. Prospects of Colloidal Nanocrystals for Electronic and Optoelectronic Applications. *Chem. Rev.* **2009,** *110*, 389.
(10) Nozik, A. J. Exciton multiplication and relaxation dynamics in quantum dots: Applications to ultrahigh-efficiency solar photon conversion. *Inorg. Chem.* **2005,** *44*, 6893.
(11) Madelung, O. M. *Semiconductors: Data Handbook*, 3rd ed.; Springer: Berlin, 2004.
(12) Walsh, A.; Watson, G. W. The origin of the stereochemically active Pb(II) lone pair: DFT Calculations on PbO and PbS. *J. Solid State Chem.* **2005,** *178*, 1422.
(13) Wei, S.-H.; Zunger, A. Electronic and Structural Anomalies in Lead Chalcogenides. *Phys. Rev. B* **1997,** *55*, 13605.
(14) Wise, F. W. Lead Salt Quantum Dots: the Limit of Strong Quantum Confinement. *Acc. Chem. Res.* **2000,** *33*, 773.
(15) Hohenberg, P.; Kohn, W. Inhomogeneous Electron Gas. *Phys. Rev.* **1964,** *136*, B864.
(16) Kohn, W.; Sham, L. J. Self-Consistent Equations Including Exchange and Correlation Effects. *Phys. Rev.* **1965,** *140*, A1133.
(17) Kresse, G.; Furthmüller, J. Efficient Iterative Schemes for Ab Initio Total-Energy Calculations Using a Plane-Wave Basis Set. *Phys. Rev. B* **1996,** *54*, 11169.
(18) Kresse, G.; Furthmüller, J. Efficiency of Ab-Initio Total Energy Calculations for Metals and Semiconductors Using a Plane-Wave Basis Set. *Comput. Mater. Sci.* **1996,** *6*, 15.
(19) Perdew, J. P.; Burke, K.; Ernzerhof, M. Generalized Gradient Approximation Made Simple. *Phys. Rev. Lett.* **1996,** *77*, 3865.
(20) Blöchl, P. E. Projector Augmented-Wave Method. *Phys. Rev. B* **1994,** *50*, 17953.
(21) Walsh, A.; Yan, Y.; Al-Jassim, M. M.; Wei, S.-H. Electronic, Energetic, and Chemical Effects of Intrinsic Defects and Fe-Doping of $CoAl_2O_4$: A DFT+U Study. *J. Phys. Chem. C* **2008,** *112*, 12044.
(22) Scanlon, D. O.; Morgan, B. J.; Watson, G. W.; Walsh, A. Acceptor Levels in p-Type Cu_2O: Rationalizing Theory and Experiment. *Phys. Rev. Lett.* **2009,** *103*, 096405.

DOI: 10.1021/jz100312y | *J. Phys. Chem. Lett.* **2010,** *1*, 1284–1287